of Table III give a much closer correlation with experimentally determined τ_Δ values, since they are derived from them, we evaluate fitted k_{XY} rate constants for the calculation of τ_Δ from the curve of Figure 6, using literature data for the highest fundamental vibrational energies of oscillators X–Y (see, for example, Table III). By comparing τ_Δ values calculated in this way with experimental values, it then becomes obvious to which extent the energy-transfer model used by us for the description of the E_{XY} dependence of k_{XY} reproduces realistic $^1O_2$ lifetimes in solution.

Figure 7 illustrates in a double-logarithmic plot the excellent correlation between calculated and experimental values. A linear least-squares fit of the data results in a straight line with slope 0.97 and intercept −0.06.

Thus the energy-transfer model proposed by us quantitatively describes the solvent dependence of the $^1O_2$ lifetime in solution. Since collisional deactivation of $^1O_2$ can occur in the gas phase and in polymers, too, our correlation may also be used for calculating lifetimes in these phases.

Conclusion

Deactivation of $^1O_2$ by solvent molecules is a collisional E → V + R + T energy transfer, which occurs by coupling of the highest fundamental vibrational mode X–Y of the acceptor molecule with an O_2 ($^1\Delta_g$, $v = 0$) → ($^3\Sigma_g^-$, $v = m$) transition. The off-resonance energy E_{ms}, which is the energy difference of the vibronic transitions in O_2 and the accepting oscillator X–Y, has to be accepted simultaneously by various other vibrational and rotational modes of the solvent molecule.

The increase of energy-transfer rate constant k_{XY} with vibrational energy E_{XY} of the highest 0 → 1 transition of oscillator X–Y is qualitatively explained by the reduction of the off-resonance energy to the various 0 → m transitions of O_2.

Quantitatively the dependence of k_{XY} on E_{XY} is given by eq 9 using an exponential correlation between off-resonance factor R_{ms} and off-resonance energy E_{ms} (eq 7).

Thus we present an energy-transfer model for the $^1O_2$ deactivation by solvent molecules which for the first time gives a reasonable physical understanding of this process *and* describes quantitatively the solvent dependence of $^1O_2$ lifetimes over more than 4 orders of magnitude.

Acknowledgment. We gratefully acknowledge financial support from the Deutsche Forschungsgemeinschaft and the Fonds der Chemischen Industrie.

Registry No. O_2, 7782-44-7; C_6F_{14}, 355-42-0; C_6F_6, 392-56-3; $CFCl_3$, 75-69-4; $C_2F_3Cl_3$, 76-13-1; CCl_4, 56-23-5; CS_2, 75-15-0; $CDCl_3$, 865-49-6.

Mechanism of Spin-State Interconversion in Ferrous Spin-Crossover Complexes: Direct Evidence for Quantum Mechanical Tunneling

Chuan-Liang Xie and David N. Hendrickson*

Contribution from the School of Chemical Sciences, University of Illinois, Urbana, Illinois 61801. *Received March 19, 1987*

Abstract: The pulsed-laser photolysis technique is used to monitor in the 300 to 4.2 K range the relaxation from the high-spin state ($^5T_2$) to the low-spin ground state ($^1A_1$) of the Fe^{II} spin-crossover complex $[Fe(6\text{-Me-py})_2(py)tren](ClO_4)_2$ doped in polystyrene sulfonate (PSS). The hexadentate ligand $(6\text{-Me-py})_2(py)tren$ is the Schiff base condensate from the reaction of 2 mol of 6-methyl-2-pyridinecarboxaldehyde, 1 mol of 2-pyridinecarboxaldehyde, and 1 mol of tris(2-aminoethyl)amine (tren). Mössbauer data for a ^{57}Fe-enriched sample of the PSS-doped complex establish that at temperatures below 340 K all of the complexes are in the low-spin state. An excitation profile obtained by monitoring the change in the electronic absorption spectrum at several different wavelengths after a single pulse of the Q-switched Nd/YAG laser establishes the fact that the phenomenon is a $^5T_2 \rightarrow {}^1A_1$ spin-crossover relaxation. At temperatures below ~120 K the relaxation rate (k) becomes relatively independent of temperature with a value of 1.4 (± 0.5) × 10^5 s^{-1} in the 50–4.2 K range. The temperature independence of the rate is direct evidence of quantum mechanical tunneling. Above ~140 K an Arrhenius plot of ln k vs. $1/T$ gives a straight line with a slope of 823 cm^{-1}. By fitting all of the 300–4.2 K relaxation rate data for the PSS-doped complex to two different theoretical models, it is shown that not only is quantum mechanical tunneling dominant at temperatures below ~120 K, but tunneling is also the predominant mechanism by which the complex makes a spin-state interconversion in the 140 to 300 K range.

Spin-crossover complexes have been reported for several different transition metals; however, those of Fe^{II} and Fe^{III} have been studied the most.[1-5] The factors which control the bulk properties (i.e., discontinuous vs. gradual) of the spin-crossover transformation in the solid state have been the main focus. On the other hand, not as much attention has been directed at understanding the dynamics and mechanism of the spin-state interconversion process. One of the reasons for this is the lack of experimental techniques which can be used to monitor directly the spin-state interconversion process in the solid state. Techniques such as Mössbauer, FTIR, and EPR spectroscopies have been used; however, the time-scale window associated with each of these techniques is very narrow. Only in the very few cases where the spin-state interconversion rate in the solid state is close to the time scale associated with a particular physical technique has it proven possible to obtain kinetic information from line-broadening studies.[6] For example, Maeda et al.[7] have very recently identified

(1) Gütlich, P. In *Structure and Bonding*; Spinger-Verlag: Berlin, 1981; Vol. 44, p 83.
(2) König, E.; Ritter, G.; Kulshreshtha, S. K. *Chem. Rev.* **1985**, *85*, 219–234.
(3) Rao, C. N. R. *Int. Rev. Phys. Chem.* **1985**, *4*, 19–38.
(4) Gütlich, P. In *Mössbauer Spectroscopy Applied to Inorganic Chemistry*; Long, G. J., Ed.; Plenum Press: New York, 1984.
(5) Gütlich, P. In *Chemical Mössbauer Spectroscopy*; Herber, R. H., Ed.; Plenum Press: New York, 1984.
(6) Goldanskii, V. I. *Pure Appl. Chem.* **1983**, *55*, 11.
(7) (a) Maeda, Y.; Tsutsumi, N.; Takashima, Y. *Inorg. Chem.* **1984**, *23*, 2440–2447. (b) Maeda, Y.; Oshio, H.; Takashima, Y.; Mikuriya, M.; Hidaka, M. *Ibid.* **1986**, *25*, 2958–2962. (c) Maeda, Y.; Takashima, Y.; Natsumoto, N.; Okyoshi, A. *J. Chem. Soc., Dalton Trans.* **1986**, 1115. (d) Matsumoto, N.; Ohta, S.; Yoshimura, C.; Ohyoshi, A.; Kohata, S.; Okawa, H.; Maeda, Y. *Ibid.* **1985**, 2575.

0002-7863/87/1509-6981$01.50/0

Fe^{III} spin-crossover complexes with variable-temperature ^{57}Fe Mössbauer spectra which exhibit line-broadening effects associated with intermediate rates of spin-state interconversion. They could estimate spin-state interconversion rates over a limited temperature range.

Even though spin-crossover complexes have been known and studied for over 50 years,[8] the most important question about these complexes has not been answered. It still remains to be determined whether an isolated spin-crossover complex either is thermally activated over a potential energy barrier in the spin-state interconversion process or quantum mechanically tunnels through the barrier.

Several groups have investigated the spin-state interconversion phenomenon in solution. In 1973 the first measurement of the rate of spin-state interconversion was reported by Beattie et al.[9] A relaxation time of 32 (±10) ns was measured for $Fe^{II}(HB(pz)_3)_2$ [$HB(pz)_3^-$ is pyrazolylborate] in CH_2Cl_2–CH_3OH solution at 25 °C employing the laser Raman temperature-jump technique. By using the same technique, Wilson et al.[10] studied several spin-crossover complexes in solution over a limited temperature range to find that (1) the kinetics of the spin-crossover process is sensitive to ligand structure where certain rigid polydentate ligands offer a "mechanical restriction" to inner-sphere reorganization; (2) Fe^{III} spin-crossover complexes interconvert faster than Fe^{II} complexes; (3) the spin-state interconversion process occurs faster in solution than in the solid state; and (4) the kinetics of the spin-state interconversion process are independent of concentration. Finally, ultrasonic absorption temperature-jump measurements were utilized by Beattie et al.[11] to measure solution relaxation rates for certain spin-crossover complexes which are too fast to monitor with the laser Raman temperature-jump technique.

Very recently the pulsed-laser photolysis technique was utilized by McGarvey and co-workers[12] to measure relatively directly the relaxation rate constant of spin-state interconversion for spin-crossover complexes in solution. A laser pulse at the wavelength of a metal-to-ligand charge-transfer (MLCT) absorption was used to excite complexes from the low-spin ground state to a MLCT excited state, whereupon a certain fraction of the complexes inter-system cross to the high-spin excited state. The electronic absorption spectrum is monitored after the laser pulse to determine the spin-state interconversion relaxation rate. From their variable-temperature work McGarvey et al.[12a,c] were able to evaluate the activation parameters for certain spin-crossover complexes in solution. For all the complexes they studied, Arrhenius behavior was observed for the temperature dependence of the spin-state interconversion rate in solution. However, data were not measured to low enough temperatures to ascertain what mechanism(s) (thermal activation over a barrier or quantum tunneling through a barrier) is (are) effective in the spin-state interconversion phenomenon. At the outset it should be emphasized that Arrhenius-type behavior can be encountered even when tunneling is dominant.[13]

In this paper results from pulsed-laser photolysis experiments carried out from 300 to 4.2 K on a Fe^{II} spin-crossover complex are presented to determine the mechanism of the spin-state interconversion. Direct evidence for quantum mechanical tunneling is presented.

Experimental Section

Compound Preparation. Elemental analyses were performed in the Microanalytical Laboratory of the School of Chemical Sciences. Commercially available tris(2-aminoethyl)amine (tren) was purified by converting it to its hydrochloride salt, followed by recrystallization in ethanol. Anal. Calcd for $N(CH_2CH_2NH_2)_3 \cdot 3HCl$: C, 28.20; H, 8.28; N, 21.91. Found: C, 28.30; H, 8.28; N, 21.88. Other commercial reagents were used without further purification.

A sample of $[Fe(6\text{-Me-py})_2(py)tren](ClO_4)_2$ was prepared by a modification of the method reported by Hoselton et al.[14] The synthesis was carried out under an argon atmosphere with Schlenkware. A 0.542-g (2 mmol) portion of tren·3HCl was dissolved in a methanol solution containing 0.34 g of $NaOCH_3$. Then 0.214 g (2 mmol) of 2-pyridinecarboxaldehyde was added to the solution. After the mixture was stirred for 20 min, 0.484 g (4 mmol) of 6-methyl-2-pyridinecarboxaldehyde was added to the solution. The Schiff base solution was further stirred for 30 min before it was transferred to a flask containing 0.40 g (2 mmol) of $FeCl_2 \cdot 4H_2O$ in methanol. A deep purple microcrystalline solid resulted after the addition of a small amount of methanol containing 1 g of $NaClO_4$. This solid was filtered off and washed with methanol, followed by drying in an argon stream. Anal. Calcd for $FeC_{26}H_{31}N_7O_8Cl_2$: N, 14.07; C, 44.85; H, 4.49; Fe, 8.02. Found: N, 13.74; C, 43.93; H, 4.51; Fe, 8.18.

An ^{57}Fe-enriched sample of $[Fe(6\text{-Me-py})_2(py)tren](ClO_4)_2$ was prepared by starting with ^{57}Fe powder (99.5% enriched, New England Nuclear). ^{57}Fe powder (20 mg) was dissolved in 10 mL of concentrated hydrochloric acid by heating at 120 °C for 5 min in an oil bath. Greenish $^{57}FeCl_3 \cdot 6H_2O$ was isolated by evaporating the solution on a rotary evaporator and this was used to prepare the ^{57}Fe-enriched compound as indicated above. Variable-temperature ^{57}Fe Mössbauer and magnetic susceptibility measurements were carried out for this ^{57}Fe-enriched sample and the results were found to be identical with those for the unenriched sample.

$[Fe(6\text{-Me-py})_2(py)tren](ClO_4)_2$ is stable not only in the solid state, but is also stable in solution in the presence of O_2. Thus, the preparation of a polymer-doped sample of this complex is straightforward. The doping into polystyrene sulfonate (PSS) film was carried out simply by dissolving both the compound and PSS in water and then allowing the solution to evaporate on a piece of glass slide. The solution to be evaporated typically contained 1 mg of the compound and 15 mg of PSS in 1 mL of H_2O. Evaporation of this solution gave a thin film of the doped polymer. For Mössbauer experiments, the film was peeled off the slide and loaded into a Mössbauer cell. For measurements of the electronic absorption spectrum in the pulsed-laser photolysis experiment, the thin film was left on the glass slide, which was loaded into the liquid-helium cryostat.

Physical Measurements. ^{57}Fe Mössbauer spectra were run on a constant-acceleration spectrometer which was described previously.[15] The estimated accuracy of absolute sample temperature determination is ±1 K below 10 K, better than ±2 K for the 20–30 K region, and ±3 K for temperatures above ~30 K. The relative precision of temperature determination is ±0.5 K at the higher temperatures. Isomer shift data are reported relative to iron foil at 298 K, but isomer shifts are not corrected for second-order Doppler effects. It should be noted that isomer shifts illustrated in the figures are displaced slightly from the actual values, whereas accurate values are to be found in the tabulated results. Computer fittings of the Mössbauer data to Lorentzian line shapes were carried out with a modified version of a previously reported computer program.[16]

Variable-temperature magnetic data were collected on a VTS-50 Series 800 SQUID susceptometer (S.H.E. Corp.) interfaced with an Apple IIe personal computer. The sample was tightly packed in a cylindrically shaped Delrin sample container with an inner diameter of about 4 mm. Sampler temperature control was achieved by means of a S.H.E. digital temperature monitor. Each data point was taken by averaging 10 measurements taken after the sample reached temperature equilibrium. Pascal's constants were employed for the value of the diamagnetic susceptibility.

Variable-temperature UV–vis electronic absorption spectra were recorded on a Varian Model 2300 UV–vis–NIR spectrophotometer with a Janis optical dewar. The optical windows of the dewar consisted of $^1/_8$

(8) (a) Cambi, L.; Cagnasso, A. *Atti Accad. Naz. Lincei, Cl. Sci. Fis., Mat. Nat., Rend.* **1931**, *13*, 809. (b) Cambi, L.; Szego, L. *Ber. Dtsch. Chem. Ges. B* **1931**, *64*, 259.

(9) Beattie, J. K.; Sutin, N.; Turner, D. H.; Flynn, G. W. *J. Am. Chem. Soc.* **1973**, *95*, 2052.

(10) (a) Dose, E. V.; Tweedle, M. F.; Wilson, L. J.; Sutin, N. *J. Am. Chem. Soc.* **1977**, *99*, 3886. (b) Hoselton, M. A.; Drago, R. S.; Wilson, L. J.; Sutin, N. *Ibid.* **1976**, *98*, 6967. (c) Petty, R. H.; Dose, E. V.; Tweedle, M. F.; Wilson, L. J. *Inorg. Chem.* **1978**, *17*, 1064. (d) Dose, E. V.; Murphy, K. M.; Wilson, L. J. *Ibid.* **1976**, *15*, 2622. (e) Reeder, K. A.; Dose, E. V.; Wilson, L. J. *Ibid.* **1978**, *17*, 1071. (f) Dose, E. V.; Hoselton, M. A.; Sutin, N.; Tweedle, M. F.; Wilson, L. J. *J. Am. Chem. Soc.* **1978**, *100*, 1142.

(11) (a) Beattie, J. K.; Binstead, R. A.; West, R. J. *J. Am. Chem. Soc.* **1978**, *100*, 3044. (b) Binstead, R. A.; Beattie, J. K.; Dewey, T. G.; Turner, D. H. *Ibid.* **1980**, *102*, 6442.

(12) (a) Lawthers, I.; McGarvey, J. I. *J. Am. Chem. Soc.* **1984**, *106*, 4280. (b) McGarvey, J. I.; Lawthers, I.; Toftlund, I. *J. Chem. Soc., Chem. Commun.* **1984**, 1576. (c) McGarvey, J. J.; Lawthers, I. *Ibid.* **1982**, 906.

(13) See, for example: DeVault, D. *Quantum-Mechanical Tunnelling in Biological Systems*; Cambridge University Press: Cambridge, 1984.

(14) Hoselton, M. A.; Wilson, L. J.; Drago, R. S. *J. Am. Chem. Soc.* **1975**, *97*, 1723.

(15) Cohn, M. J.; Timken, M. D.; Hendrickson, D. N. *J. Am. Chem. Soc.* **1984**, *106*, 6683.

(16) Chrisman, B. L.; Tumolillo, T. A. *Comput. Phys. Commun.* **1971**, *2*, 322.

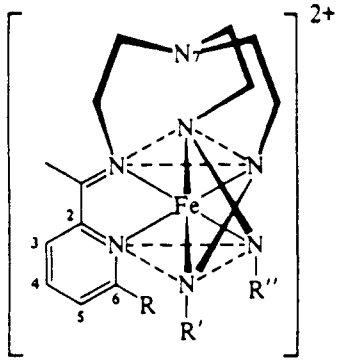

Figure 1. Schematic drawing of the molecular structure of the cation in $[Fe(6\text{-Me-py})_2(py)tren](ClO_4)_2$. R is a methyl substituent, whereas R′ and R″ stand for methyl-substituted and unsubstituted, respectively, pyridine Schiff-base arms as explicitly indicated for the one ligand arm.

in. thick fused silica and quartz plates, and they were carefully balanced by two other quartz plates in the reference beam. An L-shaped metal sample holder was used to hold the optical cell. The sample holder was attached to the tip of the shaft which came with the dewar. The metal sample holder provided sufficient heat conduction. The temperature sensor and heater were located on the tip of the shaft. A Lake Shores Model DST-80D temperature controller was used to control the sample temperature. Before each spectrum was taken, a period of 20 min was allowed for the sample to reach temperature equilibrium. A baseline recorded at room temperature with a blank solution was subtracted from each spectrum as a baseline correction. A slight baseline shift was observed as the temperature was decreased and this shift was compensated by means of a zero-point correction, which brought the absorbance of each spectrum to 0 at 800 nm.

The pulsed-laser photolysis experiments were carried out with a Q-switched Nd/YAG pulsed laser at a frequency doubling mode of 532 nm with a pulse width of 15 ns and about 50 mJ per pulse power output. The probe beam pathway consisted of a xenon flash lamp, an optical lens, a sample holder, a monochromator, and photomultiplier tube. The Nd/YAG laser and the data acquisition system were synchronized by a timing box. A Tektronix R7912 transient digitizer and a Tektronix computer were used for data acquisition and storage. Each time-resolved electronic absorption profile consisted of 512 sampling points. Each profile was stored on floppy disk and transferred to a VAX 11/780 computer for analysis. Control of the sample temperature was effected with a Janis optical dewar combined with a Lake Shores Model DST-80D temperature controller. Before each spectrum was recorded in the relaxation studies, the sample was allowed to reach temperature equilibrium for a period of 20 min. In the case of the experiments on the PSS-doped $[Fe(6\text{-Me-py})_2(py)tren](ClO_4)_2$ film, the film was left attached to the glass slide where it was formed, and the slide was clamped into a position where the film plane bisected the laser and xenon probe beams. These two beams were focused to a dimension of ~3 mm and the crossing point of the two beams was carefully placed on the film, which was ~1 mm in thickness.

Results and Discussion

Spin-Crossover Characteristics of $[Fe(6\text{-Me-py})_2(py)tren](ClO)_2$. Before the pulsed-laser photolysis results are discussed, it is important to present data which characterize the spin-crossover phenomenon in the Fe^{II} complex studied. This particular Fe^{II} complex was selected because it is stable in air, both in the solid state and in solution, and because it has been studied previously[10a] in solution by the laser Raman temperature-jump technique. The fact that the Fe^{II} cationic complex does not react with O_2 in solution as well as the spin-crossover characteristics of the complex reflect the architecture of the hexadentate ligand. The molecular structure of the cationic complex is schematically illustrated in Figure 1.

Hoselton et al.[17] have previously shown that $[Fe(6\text{-Me-py})_2(py)tren](PF_6)_2$ is a spin-crossover complex both in the solid state, as well as in acetone and Me_2SO solutions. Variable-temperature magnetic susceptibility data were measured for a microcrystalline sample of $[Fe(6\text{-Me-py})_2(py)tren](ClO_4)_2$ (data for this and three

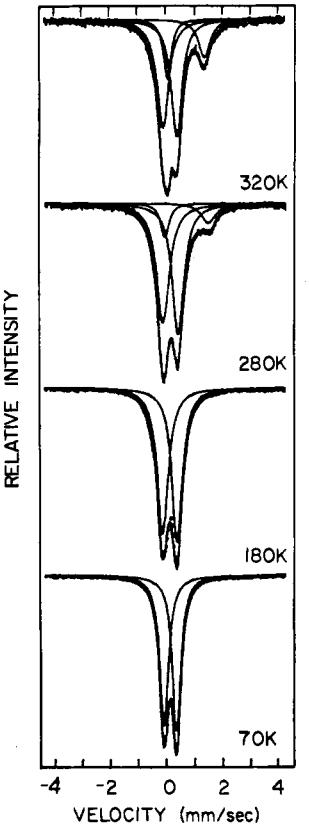

Figure 2. Variable-temperature ^{57}Fe Mössbauer spectra for $[Fe(6\text{-Me-py})_2(py)tren](ClO_4)_2$.

Table I. Mössbauer Parameters of $[Fe(6\text{-Me-py})_2(py)tren](ClO_4)_2$ from Lorentzian Fits[a]

T (K)	δ (mm/s)[b]	ΔE_Q (mm/s)[c]	$\Gamma_{1/2}(-)$[d]	$\Gamma_{1/2}(+)$[e]	f_{HS}[f]
340	0.899	1.294	0.16	0.22	0.26
	0.321	0.467	0.32	0.29	
320	0.877	1.300	0.16	0.25	0.24
	0.298	0.488	0.25	0.23	
300	0.872	1.421	0.21	0.30	0.19
	0.319	0.534	0.27	0.27	
280	0.869	1.532	0.18	0.30	0.16
	0.309	0.537	0.27	0.25	
250	0.870	1.530	0.12	0.20	0.06
	0.318	0.532	0.27	0.25	
220	0.299	0.458	0.20	0.20	0.0
100	0.298	0.444	0.18	0.17	0.0
70	0.290	0.453	0.19	0.18	0.0

[a] Fit to equal area doublets. [b] Central shift relative to iron foil at 300 K. [c] Quadrupole splitting. [d] Half-width at half-height for the left-side peaks. [e] Half-width at half-height for the right-side peaks. [f] High spin fraction estimated from the absorption area ratio.

related complexes are tabulated and illustrated in a later article). The value of μ_{eff}/Fe does not vary much from 0.36 μ_B at 10 K to 0.61 μ_B at 150 K, whereupon it gradually increases to 2.80 μ_B at 311 K. This ClO_4^- salt is also clearly a spin-crossover complex; however, the high-spin electronic state is not as thermally accessible as in the PF_6^- salt. If it is assumed[17] that μ_{eff}/Fe for a high-spin Fe^{II} complex is 5.1 μ_B and 0.45 μ_B for a low-spin Fe^{II} complex, then the ClO_4^- salt at 300 K has ~26% of the complexes in the high-spin electronic state.

^{57}Fe Mössbauer spectra were run for $[Fe(6\text{-Me-py})_2(py)tren](ClO_4)_2$ at eight different temperatures between 70 and 340 K. Selected spectra are shown in Figure 2. All spectra were least-squares fit to Lorentzian line shapes; the fitting parameters are given in Table I. From 70 to 200 K only a single quadrupole-split doublet for low-spin complexes can be seen. Above 200 K a second doublet with a quadrupole splitting characteristic of a high-spin Fe^{II} complex can be seen. The high-spin fraction (f_{HS} in Table I) estimated from the area ratio of the two doublets varies

(17) Hoselton, M. A.; Wilson, L. J.; Drago, R. S. *J. Am. Chem. Soc.* **1975**, *97*, 1722.

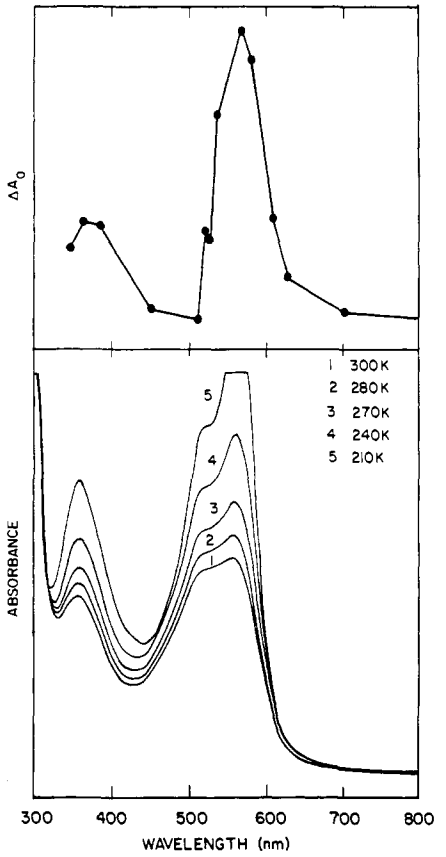

Figure 3. The lower panel shows the temperature dependence of the electronic absorption spectrum of a CH_3CN solution of $[Fe(6\text{-}Me\text{-}py)_2(py)tren](ClO_4)_2$. The upper panel shows the "excitation profile" for the laser photolysis of a CH_3CN solution of $[Fe(6\text{-}Me\text{-}py)_2(py)tren](PF_6)_2$. In this case, ΔA_0 is the change in the optical density at a particular wavelength after a single pulse of the laser.

as a function of temperature and is in qualitative agreement with the magnetic susceptibility data.

Knowledge of the UV–vis electronic absorption spectrum for the above Fe^{II} spin-crossover complex is important for the pulsed-laser photolysis experiments. Variable-temperature UV–vis spectra for an acetonitrile solution of $[Fe(6\text{-}Me\text{-}py)_2(py)tren](ClO_4)_2$ are illustrated in Figure 3. As is substantiated in a later paper, UV–vis absorption bands observed for low-spin Fe^{II} complexes are much more intense than those observed for high-spin Fe^{II} complexes. The band at 553 nm and its shoulder at 510 nm (see Figure 3) are metal-to-ligand charge-transfer (MLCT) bands of the low-spin complexes. The band at 352 nm is probably a low-spin ligand-to-metal charge-transfer (LMCT) band. Bands associated with complexes in the high-spin state are weak and masked by bands of complexes in the low-spin state. As can be seen in Figure 3, the low-spin bands increase in intensity as the temperature of the acetonitrile solution is decreased from 300 to 210 K. The increase in intensity upon decreasing the temperature obviously reflects the increase in per cent of low-spin complexes in solution as the temperature is decreased. It is clear that $[Fe(6\text{-}Me\text{-}py)_2(py)tren]^{2+}$ is a spin-crossover complex in solution.

A weak d–d transition can be seen for an acetonitrile solution of $[Fe(6\text{-}Me\text{-}py)_2(py)tren](ClO_4)_2$. A split band is seen with maxima at 892 and 907 nm (see Figure 4). This band is a d–d transition for complexes in the high-spin state. The $^5T_{2g}$ and ^5E_g states of an octahedral Fe^{II} complex are each split into two states (see Figure 4) as a result of crystal fields of symmetry lower than D_{3d}. From the energies of the 892- and 907-nm bands the crystal-field splitting parameter $10Dq$ can be determined to be 11 080 cm^{-1}. This is comparable to $10Dq$ values determined[18] for other Fe^{II} spin-crossover complexes.

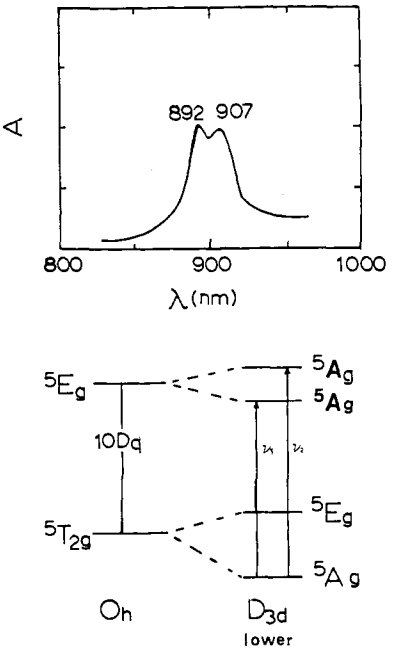

Figure 4. Electronic absorption spectrum for a CH_3CN solution of $[Fe(6\text{-}Me\text{-}py)_2(py)tren](ClO_4)_2$ in the spectral region where a d–d band for complexes in the high-spin state is seen. An energy diagram suggesting an origin for the splitting of the $^5T_{2g} \rightarrow {}^5E_g$ transition is also shown.

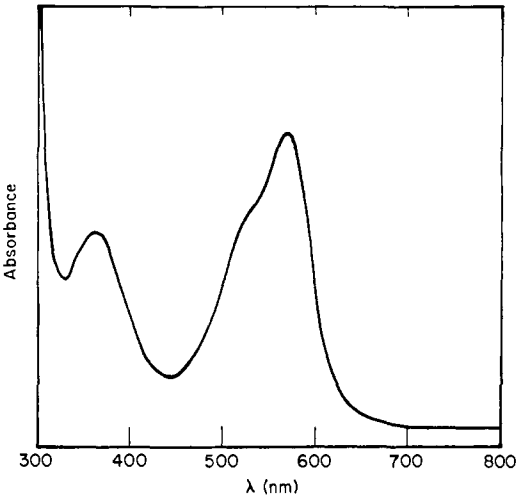

Figure 5. Room-temperature electronic absorption spectrum for PSS-doped film of $[Fe(6\text{-}Me\text{-}py)_2(py)tren](ClO_4)_2$.

In the polystyrene sulfonate (PSS) film, the high-spin state of $[Fe(6\text{-}Me\text{-}py)_2(py)tren]^{2+}$ is not thermally populated even at 340 K as judged by variable-temperature UV–vis electronic absorption and Mössbauer spectra. Very good signal-to-noise Mössbauer spectra were run from 20 to 340 K for an ^{57}Fe-enriched sample (figure showing spectra is available as supplementary material). Only one doublet characteristic of a low-spin Fe^{II} complex (ΔE_Q = 0.659 mm/s and δ = 0.358 mm/s at 340 K) could be seen at all temperatures. Similarly, there was no temperature dependence seen in the UV–vis spectrum of the polymer-doped sample. However, the spectrum of the polymer-doped complex (see Figure 5) looks very similar to the spectrum obtained for the complex in solution. The band found at 553 nm for an acetonitrile solution is red shifted to 562 nm in the PSS film, while the 352-nm solution band is blue shifted to 342 nm upon doping into the PSS film. It is clear that the $[Fe(6\text{-}Me\text{-}py)_2(py)tren]^{2+}$ cation is present in the polymer-doped sample; however, the high-spin state of this cation is at higher energies than it is in the ClO_4^- salt. There could be some specific interaction of the sulfonate group on the polymer

(18) Wilson, L. J.; Georges, D.; Hoselton, M. A. *Inorg. Chem.* **1975**, *14*, 2968.

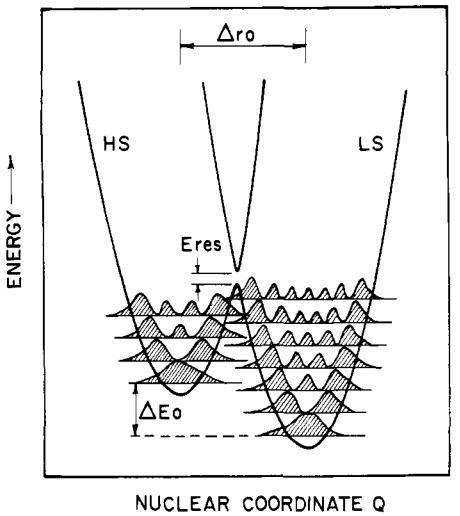

Figure 6. Simplified one-dimensional potential-energy diagram for a Fe^{II} spin-crossover complex. Vibrational levels and associated probability functions corresponding to only one mode, perhaps the symmetric metal–ligand stretching mode, are shown.

backbone with the Fe^{II} cation in a cavity of the polymer. The so-called inomer effect[19] may lead to the stabilization of the low-spin electronic state. It must be emphasized that only a small (>−200 cm^{-1}) change in the energy separation between the low-spin ground state and high-spin excited state between the polymer and ClO_4^- salt environments is needed to lead to this change.

Pulsed-Laser Photolysis Experiment. Mechanistic questions related to the spin-state interconversion process of a spin-crossover complex can be best understood by reference to a simplified one-dimensional potential-energy diagram[20] (see Figure 6). The potential energy of the complex is plotted as a function of the generalized vibrational normal coordinate involved in the spin-state interconversion. The symmetric metal–ligand stretching mode is probably the most important one involved, for there is generally an appreciable increase in the metal–ligand–atom distances as the spin-crossover complex converts from the low-spin ground state to the high-spin excited state. Other normal coordinate vibrations involving angular deformations could also be active. The singlet ground state and quintet excited state of a Fe^{II} spin-crossover complex interact via second-order spin–orbit coupling through the intermediacy of a high-energy triplet state. In Figure 6 the resonance energy E_{res} gauges the magnitude of this interaction. The value of E_{res} for a Fe^{II} spin-crossover complex has been estimated[21] to be in the range of ~100 cm^{-1}. As can be seen from Figure 6, the rate of spin-state interconversion depends on three main factors: the value of the resonance energy E_{res}; the dimensional change Δr_0; and the difference in zero-point energies, ΔE_0, between the low- and high-spin states. Obviously the last factor reflects the ligand-field strength of the ligand.

For simplicity sake only vibrational levels of one normal mode are shown for the low- and high-spin states in Figure 6. In converting from the high-spin state to the low-spin state a spin-crossover complex can either be thermally activated to overcome the potential-energy barrier or it can quantum mechanically tunnel through the barrier. The best way to discover which of these two mechanisms is important is to measure the spin-state interconversion rate as a function of temperature from 300 to 4.2 K.

The strategy of the pulsed-laser photolysis experiment is evident in the Jablonski diagram for a Fe^{II} spin-crossover complex shown in Figure 7. The frequency doubled laser pulse at 532 nm excites the Fe^{II} spin-crossover complexes from the $^1A_1$ ground state to

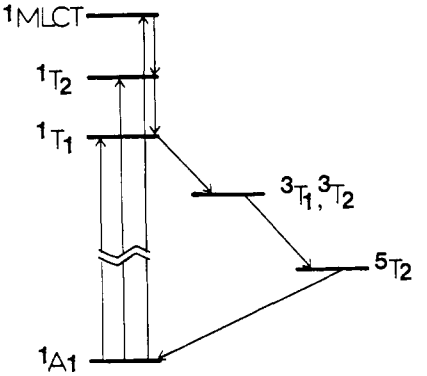

Figure 7. Jablonski diagram showing the low-spin $^1A_1$ ground state and various excited states of a Fe^{II} spin-crossover complex. The laser pulse at 532 nm excites the $^1A_1 \rightarrow {}^1$MLCT transition of the $[Fe(6\text{-Me-py})_2(py)tren]^{2+}$ complex.

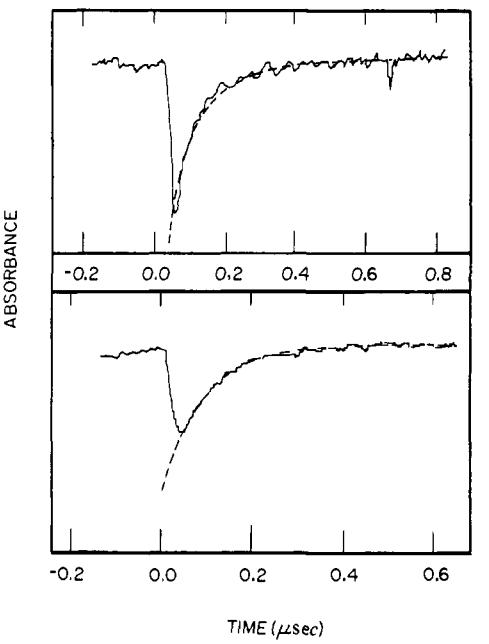

Figure 8. The lower panel shows a typical single-pulse relaxation profile for $[Fe(6\text{-Me-py})_2(py)tren](ClO_4)_2$ in CH_3CN. The change in the electronic absorption spectrum was detected at 560 nm. The dashed line resulted from a least-squares fit to a single exponential decay. The upper panel shows a typical multiple-pulse relaxation profile for $[Fe(6\text{-Me-py})_2(py)tren](ClO_4)_2$ doped in polystyrene sulfonate (PSS).

a singlet MLCT excited state. The maximum of the electronic absorption band for the $^1A_1 \rightarrow {}^1$MLCT transition is at 562 nm. Following excitation, some fraction of the molecules will intersystem cross to triplet states ($^3T_1$ and $^3T_2$) and from there to the high-spin excited state ($^5T_2$, or in lower symmetry the ^5A component). If the rates of intersystem crossing are much faster than the relaxation of the Fe^{II} complex from the high-spin $^5T_2$ state to the low-spin $^1A_1$ state, then it is straightforward to determine directly the $^5T_2 \rightarrow {}^1A_1$ relaxation rate. Before, during, and after the laser pulse the change in the electronic absorption spectrum is monitored at some wavelength. Since high-spin Fe^{II} complexes have low molar extinction coefficients in the visible range, it is easier to follow the $^5T_2 \rightarrow {}^1A_1$ relaxation by monitoring changes in the amount of low-spin complexes as reflected by changes in the intensity of the $^1A_1 \rightarrow {}^1$MLCT band.

A typical single-pulse transient profile for an acetonitrile solution of $[Fe(6\text{-Me-py})_2(py)tren](PF_6)_2$ is shown in Figure 8. In this case the change in the absorption spectrum was monitored at 560 nm. As can be seen, the 15-ns laser pulse caused a decrease in the optical density at this wavelength. After the laser pulse, the Fe^{II} complexes relax back to the $^1A_1$ ground state. The dotted line shows the result of a least-squares fit of the change in the

(19) Mattera, V. D.; Squattrito, P. J.; Risen, W. M., Jr. *Inorg. Chem.* **1984**, *23*, 3597 and references therein.
(20) Sutin, N. *Acc. Chem. Res.* **1982**, *15*, 275.
(21) Buhks, E.; Navon, G.; Bixon, M.; Jortner, J. *J. Am. Chem. Soc.* **1980**, *102*, 2918.

Table II. Variable-Temperature Relaxation Constants for Complex $[Fe(6\text{-Me-py})_2(py)tren](ClO_4)_2$

T (K)	k ($\times 10^{-5}$ s^{-1})[b]	T (K)	k ($\times 10^{-5}$ s^{-1})[b]	T (K)	k ($\times 10^{-5}$ s^{-1})[b]
300	232.7	160	6.36	50	0.150
280	146.7	140	2.76	40	0.164
260	114.0	120	1.12	35	0.129
240	71.8	100	0.809	20	0.136
220	51.7	90	0.684	15	0.113
200	28.1	80	0.424	10	0.202
180	13.5	70	0.360	4.2	0.0875
		60	0.158		

[a] PSS represents polystyrene sulfonate polymer. [b] $k = 1/\tau$, where τ is relaxation time.

optical density at 560 nm to a simple exponential decay of the form

$$\Delta A(t) = \Delta A_0 \exp(-t/\tau) \quad (1)$$

In this expression $\Delta A(t)$ is the difference between the absorption intensity at 560 nm at time t with that at infinite time (zero time is when the laser is fired). ΔA_0 represents the amplitude of the absorption change generated by the laser pulse and τ is the relaxation time (rate = $k = 1/\tau$).

An excitation profile was determined to verify that the decrease in absorption intensity at 560 nm detected above is, in fact, due to the $^5T_2 \rightarrow {}^1A_1$ relaxation. Single-pulse profiles were recorded for a CH_3CN solution of $[Fe(6\text{-Me-py})_2(py)tren](PF_6)_2$ at room temperature with the detection wavelength set at various values in the range of 300 to 800 nm. ΔA_0 values from 14 single-pulse profiles are plotted against wavelength to give the excitation profile shown in Figure 3. A comparison with the simple solution absorption spectrum (see Figure 3) for $[Fe(6\text{-Me-py})_2(py)tren](ClO_4)_2$ in CH_3CN provides strong support for the fact that the optical changes which are being observed are indeed attributable to the $^5T_2 \rightarrow {}^1A_1$ relaxation. Furthermore, it is important to note that the average relaxation time evaluated from the 14 independent single-pulse profile is 82 ns with a deviation of only 8 ns. This is consistent within experimental error with the 110 ± 25 ns relaxation time determined for $[Fe(6\text{-Me-py})_2(py)tren](PF_6)_2$ dissolved in acetone with 10% H_2O by the laser Raman temperature-jump technique.[10a]

Finally, it should be mentioned that the excited-state characteristics of $[Fe(phen)_3]^{2+}$, where phen is 1,10-phenanthroline, have been investigated[22a] to find the lifetime of the MLCT excited state is shorter than a nanosecond down to 14 K. The lifetime of the triplet spin states was found to be subnanosecond. A lifetime of a picosecond at room temperature was also reported for the excited states of $[Fe(bpy)_3]^{2+}$, where bpy is 2,2′-bipyridine.[22b,23]

Direct Evidence for Quantum Mechanical Tunneling. In order to determine whether a Fe^{II} spin-crossover complex is thermally activated over a potential-energy barrier (see Figure 6) or if it tunnels through the barrier in the $^5T_2 \rightarrow {}^1A_1$ interconversion, relaxation rate data need to be determined over a large temperature range, including temperatures in the liquid-helium range. Obviously, if the spin-state interconversion involves only a thermal activation over a barrier, then as the sample temperature is decreased the $^5T_2 \rightarrow {}^1A_1$ rate will decrease to become zero at 0 K. If a tunneling mechanism is important, the relaxation rate will become temperature independent at low temperatures and there will be a finite rate at 0 K.[13]

It was essential for the experiment to find a medium for diluting the complexes into which remains optically transparent from 300 to 4.2 K. It was found that a dilute polymer matrix forms a film which serves well as a medium for this experiment. Polystyrene sulfonate (PSS) was selected because it is soluble in water; so is the complex $[Fe(6\text{-Me-py})_2(py)tren](ClO_4)_2$. A very transparent film was formed on a quartz plate by evaporating a water solution of PSS and $[Fe(6\text{-Me-py})_2(py)tren](ClO_4)_2$.

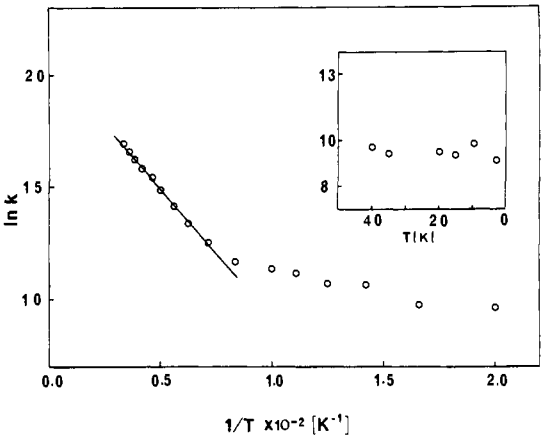

Figure 9. Plot of natural logarithm of the spin-state relaxation rate constant (k) vs. inverse absolute temperature for PSS-doped $[Fe(6\text{-Me-py})_2(py)tren](ClO_4)_2$ in the range 300 to 50 K. The inset shows k vs. temperature in the 50 to 4.2 K range. The solid line represents a least-squares fit of the 300–150 K data to a straight line with a slope of 823 cm^{-1}.

Transient profiles were determined for the PSS-doped Fe^{II} spin-crossover complex from 300 to 4.2 K. At each temperature, several single-pulse profiles were added together to improve the signal to noise. A typical profile is shown in Figure 8. As with the solution-state profile, it was possible to least-squares fit each profile to a simple exponential decay. The relaxation rates obtained in this way at temperatures from 300 to 4.2 K are given in Table II. In addition, an Arrhenius plot of ln k vs. $1/T$ is shown in Figure 9. It is seen that at temperatures above ~140 K the $^5T_2 \rightarrow {}^1A_1$ interconversion seems to exhibit an Arrhenius-type behavior, whereas, at temperatures below ~120 K the relaxation rate becomes relatively independent of temperature. The best straight line through the ln k vs. $1/T$ data in the range of 300 to 140 K has a slope of 832 cm^{-1}. As we will show in the next section, this apparent activation energy is probably not a reflection of some potential-energy barrier for thermal activation, but is due to a Boltzmann distribution of different tunneling rates from various vibrational levels. Regardless of the interpretation of the 832-cm^{-1} slope, it is clear that the relatively temperature-independent relaxation rate below ~120 K is only explicable in terms of a quantum mechanical tunneling mechanism. The relaxation rate of 1.4 (±0.5) × 10^5 s^{-1} in the 50–4.2 K range is due to Fe^{II} spin-crossover complexes tunneling from the lowest vibrational level of the high-spin state through the barrier to vibrational levels in the low-spin state (see Figure 6). It should be emphasized that the driving force, i.e., the zero-point energy difference, between these two states is not very large. Thus, the temperature independence is not a reflection of $\Delta E_0 = \lambda$, where λ is the reorganization energy.

Theoretical Analysis of Relaxation Rates. A fitting of the 300–4.2 K relaxation rate data for the PSS-doped spin-crossover complex to theoretical models for tunneling can give insight about the origin of the 823-cm^{-1} apparent activation energy. Two different theoretical models were selected for this purpose.

Following Förster's electron-transfer theory, Hopfield[24] developed an equation for the rate of electron tunneling between two fixed sites. The molecular system is interconverting between two states which are only very weakly interacting with each other. Only one vibrational mode is considered for each of the two states. The equation derived by Hopfield for thermally averaged quantum tunneling is obviously applicable to the present case where the spin-crossover complex is interconverting between two spin states.

(22) (a) Bergkamp, M. A.; Brunschwig, B. S.; Gutlich, P.; Zetzel, T. L.; Sutin, N. *Chem. Phys. Lett.* **1981**, *81*, 147. (b) Creutz, C.; Chou, M.; Netzel, T.; Okumura, M.; Sutin, N. *J. Am. Chem. Soc.* **1980**, *102*, 1309.

(23) Kirk, A. D.; Hoggard, P.; Porter, G. B.; Rockley, M.; Windsor, M. *Chem. Phys. Lett.* **1976**, *37*, 199.

(24) Hopfield, J. J. *Proc. Natl. Acad. Sci. U.S.A.* **1974**, *71*, 3640.

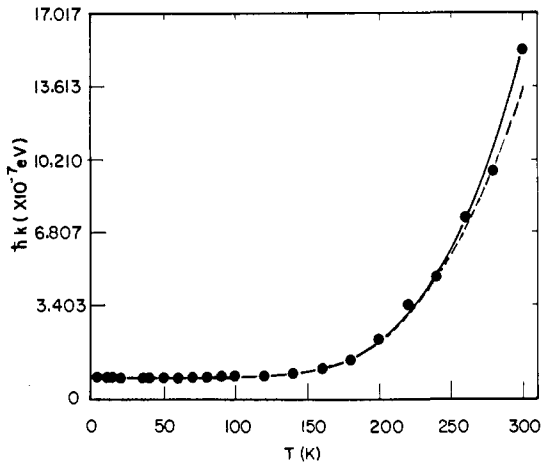

Figure 10. Plot of the spin-state relaxation rate constant vs. temperature for PSS-doped [Fe(6-Me-py)$_2$(py)tren](ClO$_4$)$_2$. Experimental data points are indicated by filled circles; the least-squares fit to Hopfield's eq 2 is given as a solid line; the least-squares fit to Jortner's eq 5 is given as a dashed line. See text for parameters.

Hopfield's equation for the rate, w_{ab}, of tunneling between two states a and b, each with one vibrational mode active, is

$$w_{ab} = \frac{2\pi}{\hbar}|T_{ab}|^2\left(\frac{1}{2\pi\sigma^2}\right)^{1/2} \exp[-(E_a - E_b - \Delta)^2/2\sigma^2] \quad (2)$$

where

$$\sigma^2 = \left(\frac{k_a X_a^2}{2}\right)(k_B T_a)\coth\left(\frac{T_a}{2T}\right) \quad (3)$$

and

$$\Delta = \tfrac{1}{2}k_a X_a^2 + \tfrac{1}{2}k_b X_b^2 \quad (4)$$

In these equations, T_{ab} is the tunneling matrix element, k_B is Boltzmann's constant, T_a ($\hbar\omega_a/k_B$) is the temperature equivalent of the quantum of the active vibrational mode which is assumed to be the same in the states a and b, ($E_a - E_b$) is the difference in zero-point energies of the two states, and $^1/_2k_aX_a^2$ reflects the reorganization energy for converting from state a to state b along the electronic potential-energy curve of state a.

It is important to note that in employing eq 2 and 3 we are assuming that the active mode in states a and b has the same quantum. The eigenvalues of the vibrational modes which are active in the spin-state change do change somewhat when the Fe^{II} complex converts from the low-spin to the high-spin state; however, the percent change is not large.[25] In solution the high-spin state of [Fe(6-Me-py)$_2$(py)tren]$^{2+}$ is thermally accessible (vide supra). Thus, it seems that the difference in zero-point energies, ΔE_0 in Figure 6, should not be too large for the PSS-doped Fe^{II} complex, even though there is no evidence in the Mössbauer spectra of population in the high-spin state at 340 K. Again, in order to minimize the number of parameters we elected to keep ΔE_0 ($=E_a - E_b$) fixed as 0.05 eV (400 cm^{-1}). The parameter ΔE_0 is only strongly coupled to the parameter Δ; variations of ΔE_0 do not appreciably influence either T_{ab}, T_a, or T_b. With these two simplifications, there are only three parameters employed in a fitting to eq 2: T_{ab}, T_a ($=T_b$), and Δ.

In Figure 10 the solid line represents a least-squares fit of the relaxation rate data to eq 2. As can be seen, the fit is quite good. What is even more impressive is that the fitting parameters are quite reasonable. With the two assumptions made above the fitting parameters are found to be T_{ab} = 52.8 cm^{-1}, T_a = 283 K (198 cm^{-1}), and Δ = 0.760 eV. In the case of a Fe^{II} spin-crossover complex, the parameter T_{ab} gauges the magnitude of the interaction between the $^1A_1$ and $^5T_2$ states. It is equivalent to E_{res} in Figure 6. The $^1A_1$ and $^5T_2$ states interact via a second-order spin–orbit interaction. The 52.8-cm^{-1} value for T_{ab} is of a reasonable magnitude for second-order spin–orbit interaction between the $^1A_1$ and $^5T_2$ states.[21]

The 197-cm^{-1} value for T_a is also in good agreement with expectations, for the predominant vibrational modes which couple to the spin-state interconversion are the metal–ligand symmetric stretching and deformation vibrations. Symmetric Fe–N stretching vibrations are expected to be in the 200–400-cm^{-1} region.[25] The reorganization energy parameter Δ can be estimated from the frequency of the symmetric Fe–N stretching vibration. By assuming $h\nu$ = 400 cm^{-1}, a reduced mass of 14 atomic units associated with ν_{Fe-N} and Δr_0 = 0.2 Å[17,26] (see Figure 6), we can calculate $\Delta = k(\Delta r_0)^2$ = 0.35 eV, which is only qualitatively in agreement with the Δ value obtained from the least-squares fitting to eq 2. However, Δ is poorly determined in this fitting procedure because it is strongly correlated with the ΔE_0 parameter which was assigned a value of 400 cm^{-1}.

Jortner et al.[21] described the spin-crossover phenomenon in solution in terms of a radiationless multiphonon process occurring between two distinct (zero order) spin states which are characterized by different nuclear equilibrium configurations separated by a potential-energy barrier which is large relative to the thermal energy k_BT. They assumed that the spin-state interconversion is nonadiabatic and employed the "Golden rule" with total wavefunctions as products of an electronic wave function and nuclear wave function both for the internal modes of the complex as well as the solvent modes to derive an expression for the rate constant k for spin-state interconversions as

$$k = (2\pi/\hbar)g_f|V|^2G \quad (5)$$

In this expression g_f is the degeneracy change in converting from the low-spin to the high-spin state, i.e., $g_f = g_{HS}/g_{LS}$. $|V|$ represents the magnitude of the coupling between the initial state Ψ_i', and the final state Ψ_f' (analogous to T_{ab} above) caused by the spin–orbit interaction operator. In eq 5 the contribution of the solvent and metal–ligand vibrational modes is given by the thermally averaged nuclear Franck-Condon vibrational overlap factor G. In order to get an analytical expression for G a relatively simple model of the vibrational modes was assumed. The solvent was represented by very low frequency oscillators, and it was assumed that only one metal–ligand vibrational mode (same frequency in both states) coupled to the spin-state interconversion to derive an expression for G (see ref 21).

In the case of an octahedral Fe^{II} spin-crossover complex, the only state which has nonvanishing spin–orbit matrix elements with both the $^1A_{1g}$ and $^5T_{2g}$ states is the $^3T_{1g}$ state from the intermediate electron configuration $t_{2g}^5e_g^1$. In this case the electronic coupling term V is given as:

$$V = -3\sqrt{2}\xi^2\left(\frac{1}{\Delta E_1} + \frac{1}{\Delta E_2}\right) \quad (6)$$

where ξ is the spin–orbit coupling constant, ΔE_1 is the energy difference between the $^3T_{1g}$ and $^1A_{1g}$ states at the equilibrium configuration of the $^1A_{1g}$ state, and ΔE_2 is the energy difference between the $^3T_{1g}$ and $^5T_{2g}$ states at the equilibrium configuration of the $^5T_{2g}$ state. As indicated above for the discussion of T_{ab}, V is of the order of 100–200 cm^{-1} for a Fe^{II} spin-crossover complex.

In fitting the spin-state relaxation rate constant data to the expanded version of eq 5 given explicitly in ref 23, the value of g_f was taken as 5 and the parameters included δ, ΔE_1, ΔE_2, $\hbar\omega$, p, and S. The parameters $\hbar\omega$, p, and S are part of the expression for the vibrational overlap factor G derived by Jortner et al.[21] The one active metal–ligand vibrational mode is characterized by $\hbar\omega$, p ($=\Delta E_0/\hbar\omega$) is simply the reduced value of the zero-point energy difference, and the coupling parameter S measures the contribution

(25) Ferraro, J. R. *Low Frequency Vibrations of Inorganic and Coordination Compounds*; Plenum Press: New York, 1971.

(26) (a) Cecconi, F.; Di Vaira, M.; Midollini, S.; Orlandini, A.; Sacconi, L. *Inorg. Chem.* **1981**, *20*, 3423. (b) Katz, B. A.; Strouse, C. E. *J. Am. Chem. Soc.* **1979**, *101*, 6214. (c) Mikani, M.; Konno, M.; Saito, Y. *Acta Crystallogr., Sect. B: Struct. Crystallogr. Cryst. Chem.* **1980**, *36*, 275.

of the change in the metal–ligand vibrational mode,

$$S = m\omega(\Delta r_0)^2/2\hbar \quad (7)$$

where m is the reduced mass.

Since from the solution study it is known that ΔE_0 is comparable to $\hbar\omega$, we decided to fix p as -1. This left five parameters. In Figure 10 the dashed line represents the best fit of the relaxation rate constant to the equation derived by Jortner et al.[21] As can be seen, not only is the relatively temperature-independent rate below ~120 K accommodated well by this treatment, but the rate data above 140 K are also accounted for. The parameters for this fit are $\xi = 164$ cm^{-1}, $\Delta E_1 = 1.05 \times 10^4$ cm^{-1}, $\Delta E_2 = 1.94 \times 10^4$ cm^{-1}, $\hbar\omega = 290$ cm^{-1}, and $S = 18.2$. For a gaseous free Fe^{II} ion, $\xi = 400$ cm^{-1}. The introduction of ligands reduces the value of ξ due to covalent interactions, and a value of $\xi = 164$ cm^{-1} is not unreasonable for a Fe^{II} complex. The quantum for the single active metal–ligand vibrational mode came out as $\hbar\omega = 290$ cm^{-1}, which is very close to what was obtained in the fitting to Hopfield's theory. The values of ΔE_1 and ΔE_2 are also reasonable, for the difference of these two numbers gives 8860 cm^{-1} for a value of $10Dq$. From the analysis of the solution electronic absorption spectrum we estimated (vide supra) $10Dq = 11\,000$ cm^{-1}. Finally, if we assume $\Delta r_0 = 0.2$ Å for a Fe^{II} spin-crossover complex, $\hbar\omega = 400$ cm^{-1}, and $m = 14$, a value of $S = 20$ can be calculated by using eq 7. This is comparable to the value of 18.2 obtained from the fit.

Concluding Remarks

Pulsed-laser photolysis experiments in the range of 300–4.2 K clearly indicate that a polymer-doped high-spin Fe^{II} spin-crossover complex employs a tunneling mechanism at temperatures below ~140 K to convert to the low-spin ground state. The relatively temperature-independent rate of $^5T_2 \rightarrow {}^1A_1$ interconversion in the low-temperature region establishes this. Furthermore, theoretical analysis of the relaxation rate data measured in the 300–4.2 K region, employing two different theoretical models, suggests that a significant contribution to the rate of spin-state interconversion above 140 K is also due to quantum mechanical tunneling. That is, the apparent activation energy of 823 cm^{-1} taken from the ln k vs. $1/T$ plot for data in the 150–300 K range is *not* simply a reflection of high-spin Fe^{II} complexes becoming thermally activated over a 823-cm^{-1} barrier. Instead, high-spin Fe^{II} complexes experience a greater tunneling rate in the $v = 1$ (assuming one active mode) vibrational level than in the lowest energy $v = 0$ level. The tunneling rate for high-spin complexes in the $v = 2$ level would be even greater than in the $v = 1$ level. When the sample temperature is increased above ~140 K a certain fraction of the high-spin molecules populate the $v = 1$ level, in addition to the $v = 0$ level. The apparent activation energy of 823 cm^{-1} reflects a Boltzmann distribution of complexes in different vibrational levels, each level with its intrinsic rate of tunneling.

Obviously considerably more laser photolysis data measured over a large temperature range down to 4.2 K are needed for spin-crossover complexes. The generality of the observation reported in this paper needs to be checked for other Fe^{II} as well as Fe^{III} and Co^{II} spin-crossover complexes. The beauty of these spin-crossover complexes of Fe^{II} (and Fe^{III}) is that there is a large flexibility in modifying these complexes. The zero-point energy difference ΔE_0 can be changed fairly easily by introducing substituents on the ligand. By changing the ligands it should be possible to systematically change the electronic coupling term (E_{res} in Figure 6) and keep the other factors relatively constant. In the case of Fe^{III} complexes, spin-crossover complexes can be obtained with S_6, Se_6, S_3O_3, and N_4O_2 ligand atom sets. These ligand-atom changes, together with variable trigonal twists enforced by ligand architecture, can be used to vary E_{res} ($\equiv V$). By varying the relative flexibility of a ligand, e.g., hexadentate vs. bis(tridentate), the vibronic coupling can be changed, which is to say that the barrier thickness can be modulated. Finally, the effect of the environment on the rate of spin-state interconversion should be probed. This issue is addressed in the following paper.

It is important to draw attention to the markedly different results on spin-crossover complexes which were recently reported by Gütlich et al.[27] and Herber and Casson.[28] They found that, upon exposure to light (xenon lamp) for a period of several minutes, crystalline samples of Fe^{II} spin-crossover complexes maintained at temperatures near to liquid-helium temperatures could be completely converted from low spin to high spin. The phenomenon was described as "light-induced excited-spin-state trapping (LIESST)". What is so remarkable is that once these Fe^{II} complexes are converted to the high-spin state they will remain in the high-spin state for hours or even days if the sample is maintained at low temperatures. Thus, the rate of $^5T_2 \rightarrow {}^1A_1$ relaxation in this case is slower by a factor of more than 10^7 than the value of $k = 1.4\ (\pm 0.5) \times 10^5$ s^{-1} we found for PSS-doped $[Fe(6\text{-Me-py})_2(py)tren](ClO_4)_2$ in the range of 50 to 4.2 K. Obviously the difference lies in the fact that we are examining the behavior of isolated Fe^{II} complexes which tunnel from the $^5T_2$ to the $^1A_1$ state. In the case of the LIESST experiments the Fe^{II} complexes are in a crystalline environment and there is cooperativity. It is likely that owing to intermolecular interactions in the crystalline environment regions (domains) of Fe^{II} complexes interconvert together. The kinetics which are being experienced are those associated with first- or higher-order phase transitions. The results of a very recent paper[29] where the LIESST phenomenon was studied as a function of x in $[Zn_{1-x}Fe_x(ptz)_6](BF_4)_2$ (ptz = 1-propyltetrazole) support this proposal.

Acknowledgment. We are grateful for support from National Institutes of Health Grant HL13652 and to Professor Peter G. Wolynes for helpful discussions.

Supplementary Material Available: Figure 1S which shows ^{57}Fe Mössbauer spectra for PSS-doped $[Fe(6\text{-Me-py})_2(py)tren](ClO_4)_2$ (1 page). Ordering information is given on any current masthead page.

(27) (a) Decurtins, S.; Gütlich, P.; Köhler, C. P.; Spiering, H.; Hauser, A. *Chem. Phys. Lett.* **1984**, *105*, 1. (b) Decurtins, S.; Gütlich, P.; Hasselbach, K. M.; Hauser, A.; Spiering, H. *Inorg. Chem.* **1985**, *24*, 2174.
(28) Herber, R.; Casson, L. M. *Inorg. Chem.* **1986**, *25*, 847.
(29) Hauser, A.; Gütlich, P.; Spiering, H. *Inorg. Chem.* **1986**, *25*, 4245.